International Conference `Wind Effects on Trees'
September 16-18, 2003, University of Karlsruhe, Germany

THE INFLUENCE OF AERODYNAMIC PROPERTIES OF FOREST EDGES AND STANDS ON THE PRESSURE PATTERN WITHIN A FOREST

W. Agster and B. Ruck

University of Karlsruhe, Laboratory of Building- and Environmental Aerodynamics, Institute for Hydromechanics

Abstract

Detailed pressure measurements have been carried out inside model forest stands in an atmospheric boundary layer wind tunnel. The experiments showed a close link between parameters such as edge angle and edge porosity with the pressure distribution inside the forest. Various leading and trailing edge geometries with angles ranging from 45...80° and optical porosity between 0.08...0.23 were tested. It was found that the steeper the edge angle the greater and the longer will be the zone of impact pressure inside the forest starting from right behind the leading edge. The area distribution of positive pressure coefficient (pressure higher than the ambient pressure) and negative pressure coefficient (suction) is influenced significantly by the leading edge angle of the forest. It was found that the leading edge region up to a distance of 1...1.5 h is characterized by significant pressure gradients acting on the trees, both, in vertical and horizontal direction.

Introduction

The susceptibility of vast homogeneous stands, especially Norway spruce *Picea abies* is well-known (von Fürst 1912). This is especially true on wet soils (Hütte 1967, Prien & Leydolph 1974, Wangler 1976), where only shallow root systems are developed and vitality may be reduced. Contrary to untreated spruce stands with increasing stability (in terms of h/d-value) of superiour trees with age (Weihs et al. 1999), homogenous stands raised according to growth tables (Wiedemann in Schober 1995) retain very unstable h/d-values (between 80-110) within the life span of 120 years, with a typical peak, i.e. a maximum instability, around age 50 (first yield class) at 20 m stand height. Taking into account vast clear-cut areas in German forests as consequence of World War II and reforestation with spruce from 1950, there is maximum instability of many such stands at age 45-50 and coincidence with the severe storm (called `Lothar') on December 26, 1999, causing a damage of 20 million m^3 in the state of Baden-Württemberg. Homogeneous, unstable stands, on huge areas are prone to catastrophe. Under these vulnerable circumstances, collective aerodynamic properties play a crucial role. Of special importance is the leading edge which can be considered as a step change in surface roughness and will influence properties of the turbulent flow above and within the forest (Fraser 1964, Irvine et al. 1997, Agster & Ruck 2002, Morse et al. 2002). Ruck & Adams 1991 showed in a wind tunnel simulation that shortly behind a leading forest edge turbulent flow quantities are peaked close to the canopy, see fig.1. Often, characteristic pattern of windthrow with remaining stand edges (not necessarily comprising only the more stable outermost one or two rows of trees) are observed in forests and field crop as well

(Fritzsche 1933, Vogl 1912), see fig.2. The governing effects therefore seem to be of very fundamental nature, not too sensible with regard to the type of canopy.

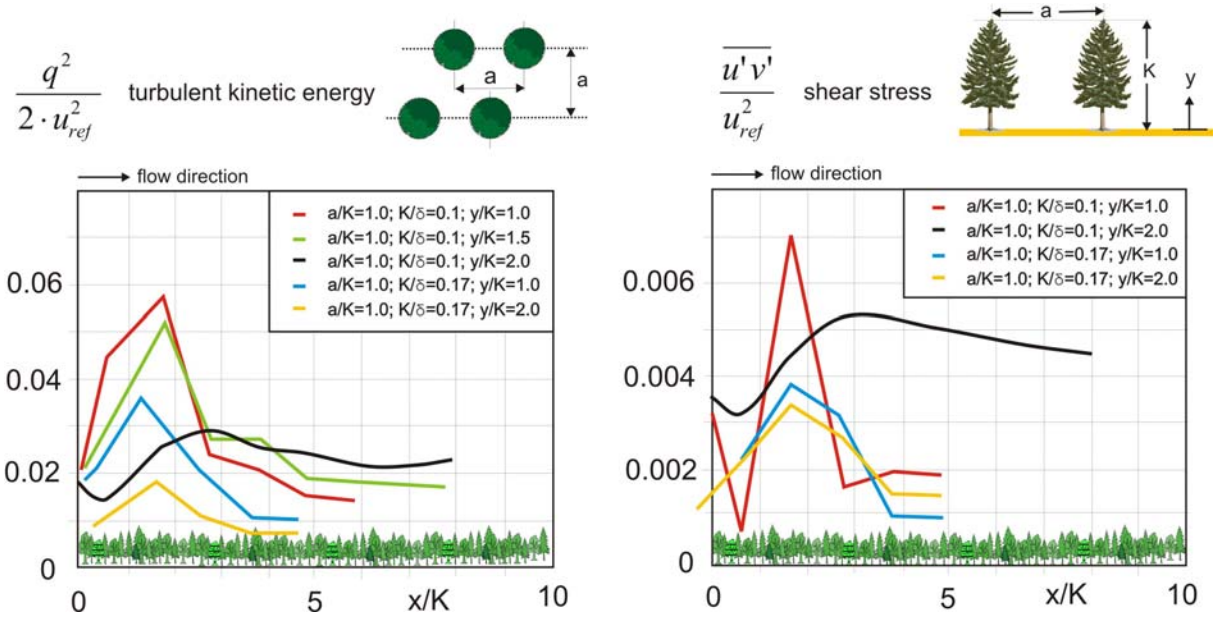

Fig. 1: Streamwise development of turbulent kinetic energy and shear stress after the forest edge at different heights above treetop level (Ruck & Adams, 1991)

Different types of forest edges include also flat edges consisting of different species of trees and shrubs, strong individuals of the main tree species or trees of the former center of a stand after windthrow or clear-cutting (see Schretzenmayer et al. 1974). In this work, edge parameters like angle and porosity have been chosen to illustrate the edge's influence on patterns of pressure within the forest. These patterns are known to be linked to the airflow above (Sigmon et al. 1983). Experiments were conducted in a simulated surface layer using model forests at scale 1:200 in an open-circuit wind tunnel. Pressure measurements were carried out using standard pressure tapping technique.

Figure 2: Similar pattern of wind damage in a forest and corn field, respectively. Note remaining edges.

Experimental details

The experiments were performed in an open circuit wind tunnel (type Göttingen). The wind speed profile was adjusted to α = 0.26 (from power law, see fig. 3), using spires (Counihan 1969) and roughness elements as usually applied to simulate atmospheric surface layer profiles in wind tunnels.

The model forest consists of an array of 400 evenly-spaced trees, forming a rectangular forest stand of 50 cm by 60 cm. The trees are mounted on wooden ballasted spheres enabling limited dynamical response of the trees. For the experiments on pressure shown here, significant deflection has been avoided by the choice of an appropriate wind speed. The distance of a given tree to it's nearest six neighbours is 26 mm each, the canopy closure is about 50 %, which is a compromise between a dense canopy and the space necessary to allow sway. In order to suppress three-dimensional flow field disturbances caused by entrainment effects into the open test section the model forest is bordered by splitter plates, 2h in height. The model forest remained unchanged throughout the experiments.

The forest edges were simulated by open cell polyurethane foam with a standardised density of about 10 pores per inch (ppi). The material was cut to long wedges with triangular cross-sections of different angles as to simulate different forest edge shapes. As known from vegetative forest edges, the angle β influences the porous volume V and thus optical porosity Φ and real permeability as well. Further, the open cell foam creates a rough surface of length c which also depends on β. The parameters for the forest edges are shown in tab. 1. The profiles of optical porosity Φ are given in fig. 4.

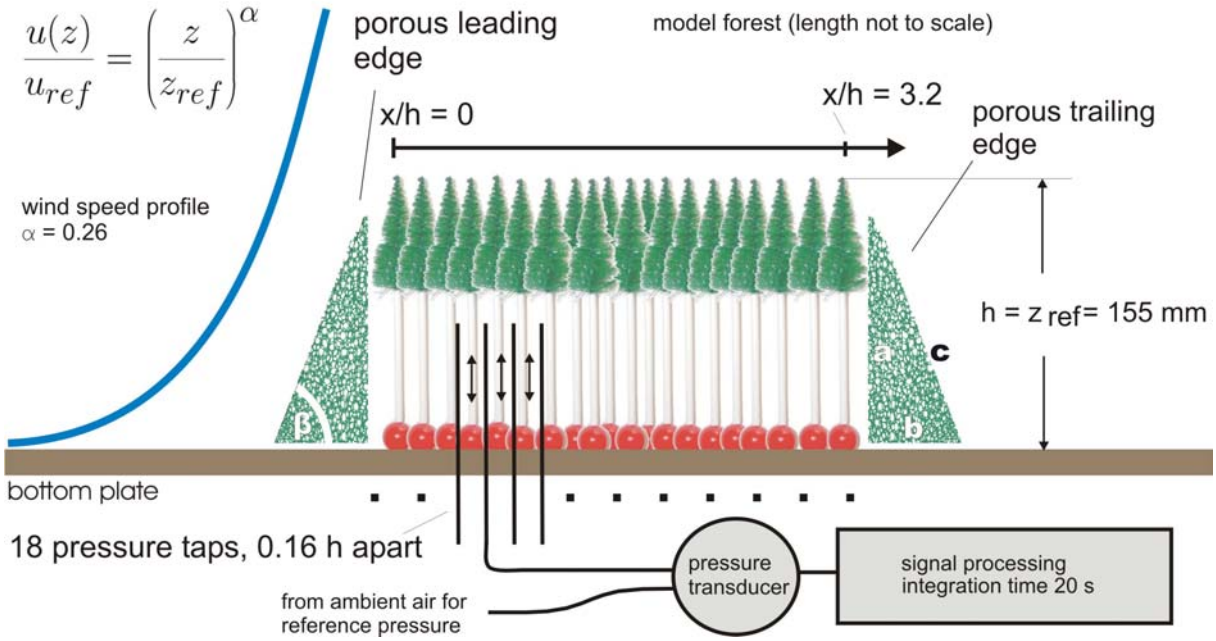

Figure 3. Experimental setup inside the wind tunnel with model forest, variable leading and trailing edges and measuring equipment.

Table 1. Model forest edges (10 ppi PU foam) and their characteristic parameters.

β [°]	a [mm]	b [mm]	c [mm]	cross-sectional area A [mm²]	Φ
80	120	21	122	1270	0.23
70	120	44	128	2621	0.20
60	120	69	139	4157	0.12
45	120	120	170	7200	0.08

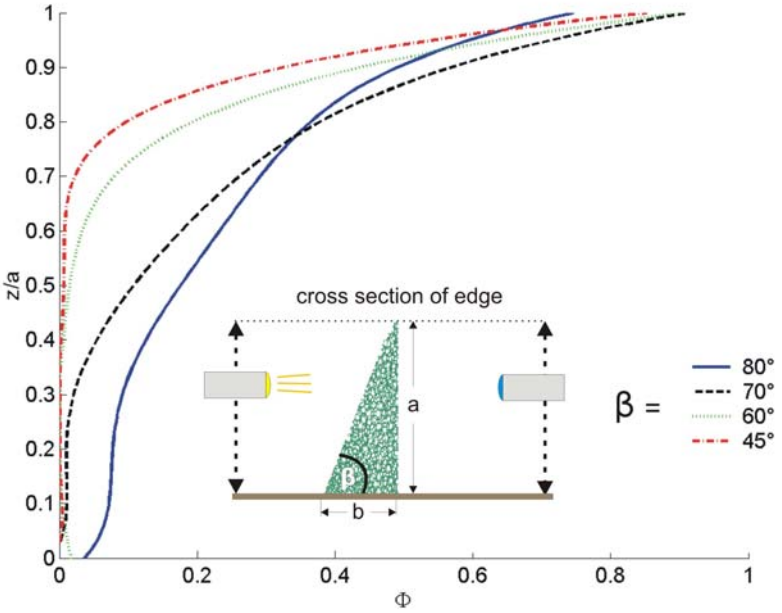

Figure 4: . Vertical profiles for optical porosity Φ of edge models with varied angle, as determined photographically. Note: the 80° curve theoretically should not cross the other. Deviation is due to difficulties in slicing the material at sharp angles.

Pressure measurements

18 pressure taps were evenly spaced along the model forest's center line, each 0.16 h or 25 mm apart, covering a range of 0.32..3.1 x/h. These pressure taps were adjusted to measuring heights z from 0...170 mm in steps of 10 mm. These correspond to 0...1.1 tree heights. This resulted in a grid of 18 by 18 = 324 measured points within the center plane. Pressure values were taken as difference between static pressure p_1 inside the model forest and ambient pressure p_0 using a pressure transducer. An Integration over 20 sec per point was performed. The static pressure differences are given normalized with the dynamic pressure at reference height z_{ref} in the approach flow delivering dimensionless (static) pressure coefficients c_{ps}. The reference speed u_{ref} in reference height z_{ref} = h was measured with a hot-wire anemometer and kept constant at 8.5 m/s.

$$c_{ps} = \frac{p_1 - p_0}{(\rho/2)\cdot u_{ref}^2}$$

It should be noted that the pressure taps are small tubes inserted perpendicular to the horizontal axis and to the main flow direction. The results might be influenced by the variation of local flow direction inside the porous media at a given point, however, potential measuring errors will be smoothed by the great number of measuring points.

Results

Airflow through and around forest canopies is characterized by accelerated air masses above the edge and a secondary flow within the trunk space below the canopy (e.g. Shaw 1977). This is most clearly shown in the setup with no leading nor trailing edge (fig. 5). Obvious is an area of high pressure at the windward edge, reaching up to ca. 0.8 z/h (with the base of the canopy at 0.6 z/h). There is also high pressure within the crown space of the first trees up to 1.5 x/h. The trunk space is characterized by a low pressure space, which is well-distinct from the crown space within the range x/h = 0...1.5 and heightens leewards, due to suction at the open trailing edge.

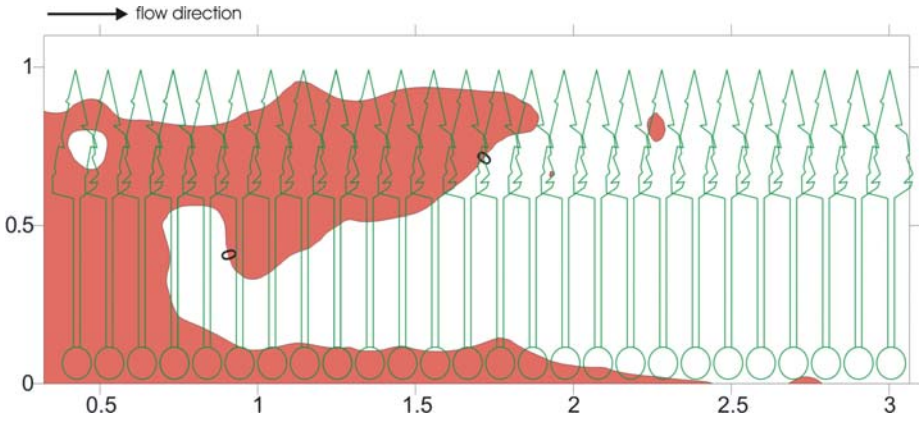

Figure 5. Zone of positive pressure coefficients c_{ps} in the edge-near region (coloured area); model forest with free airflow through the trunk space

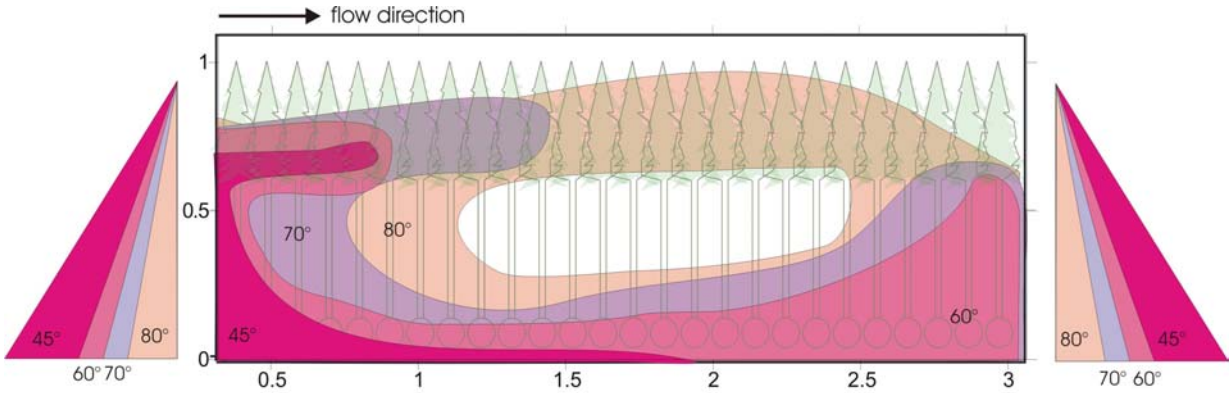

Figure 6. Zone of positive pressure coefficients inside the forest (coloured area) as a function of forest edge angle (45° to 80°, see tab. 1 for details); smoothed data.

The experiments with variable edges deliver remarkable results showing, first of all, that the application of permeable edges of different angles (fig. 6) does not principally change the shape of the pressure pattern inside the forest near the leading edge. The pattern of positive pressure coefficients c_{ps} resembles to a “C”. Apparently, there is a zone of positive pressure coefficients in the canopy starting directly from the edge. The C-type pattern is stretched into the forest in streamwise direction as a function of edge angle. As can be seen, the region near the forest edge is characterized by significant pressure gradients in horizontal and in vertical direction.

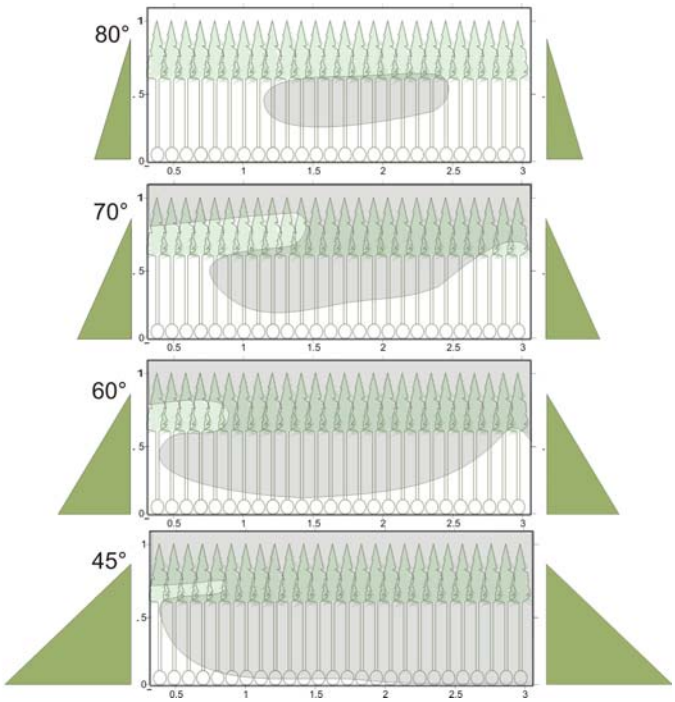

Fig.7: Zones of negative pressure coefficients inside the forest (shaded area) as a function of forest edge angle

The latter can be confirmed by numerical computations, see fig. 8 and 9, where a forest model was exposed to a numerically simulated atmospheric boundary layer. As can also be seen in fig. 7, for all investigated edge shapes, also the complementary zones of negative pressure coefficients exist. With a steepening of the forest edge, these areas are reduced in size inside the forest and shifted in streamwise direction, see fig.7. At the end of the forest near the trailing edge, afflux causes a rise in pressure, which is due to the fact that the edge itself has a higher flow resistance than the branch free trunk space.

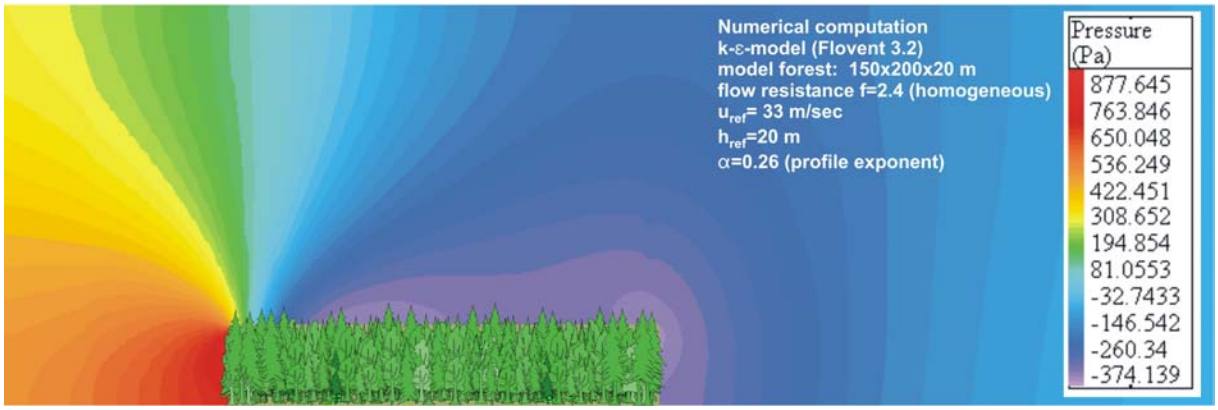

Fig. 8: Numerical computation of the pressure field around a small forest stand, 90°-edge

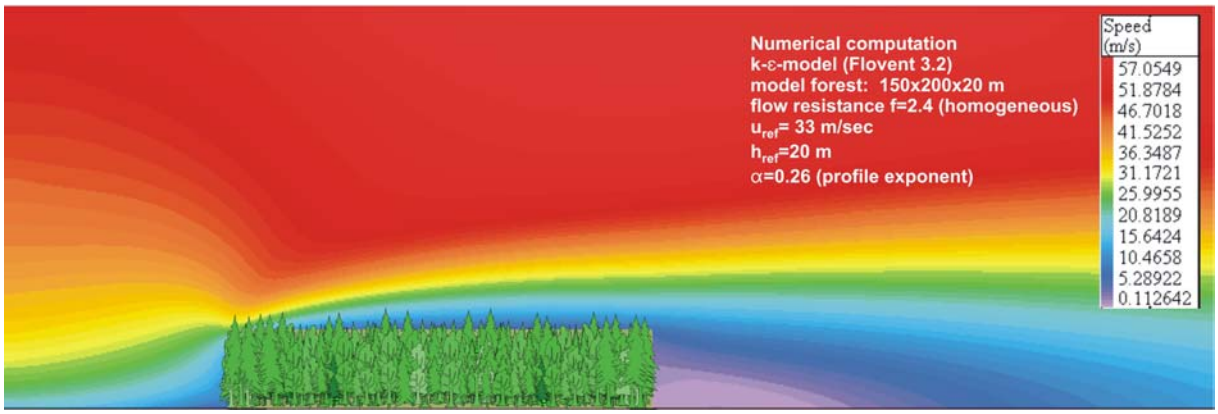

Fig. 9: Numerical computation of the velocity field around a small forest stand, 90°-edge

As might be inferred from fig. 7, the 45° edge seems to give the best shelter for the model forest stand. For the given permeability (or effective porosity) of the material used at given speed, the edge at angle 45° provides a quite homogeneous pressure pattern within the forest, indicating a high degree of shelter and little permeability.

The data presented in fig. 5-7 and table 2 respectively, compare areas of positive and negative pressure coefficient. They clearly show, that steep forest edge angles β (coinciding with higher optical porosity Φ) cause larger areas of higher pressure within the model forest when compared to shallow angles.

Table 2. Areas of positive pressure coefficient c_{ps} for different model forest edges.

β [°]	no edge	80°	70°	60°	45°
Φ	1.00	0.23	0.20	0.12	0.08
extent [x/h]	1.9	2.7	1.5	0.8	0
area	35.4 %	63.3 %	46.0 %	26.0 %	4.0 %

Pressure differences along lines of constant height (canopy z/h = 0.7 and trunk space z/h = 0.4) reflect the aforementioned findings, see fig. 10. A remarkable difference can be seen between forests with edges and a forest with no edge (free flow into the trunk space), where a significant pressure drop near the leading edge occurs. The zone of this pressure drop reaches to about x/h =1. For the forests with edges, the measured differences of pressure coefficients along level A and B are relatively small shifting slightly from negative values to positive ones

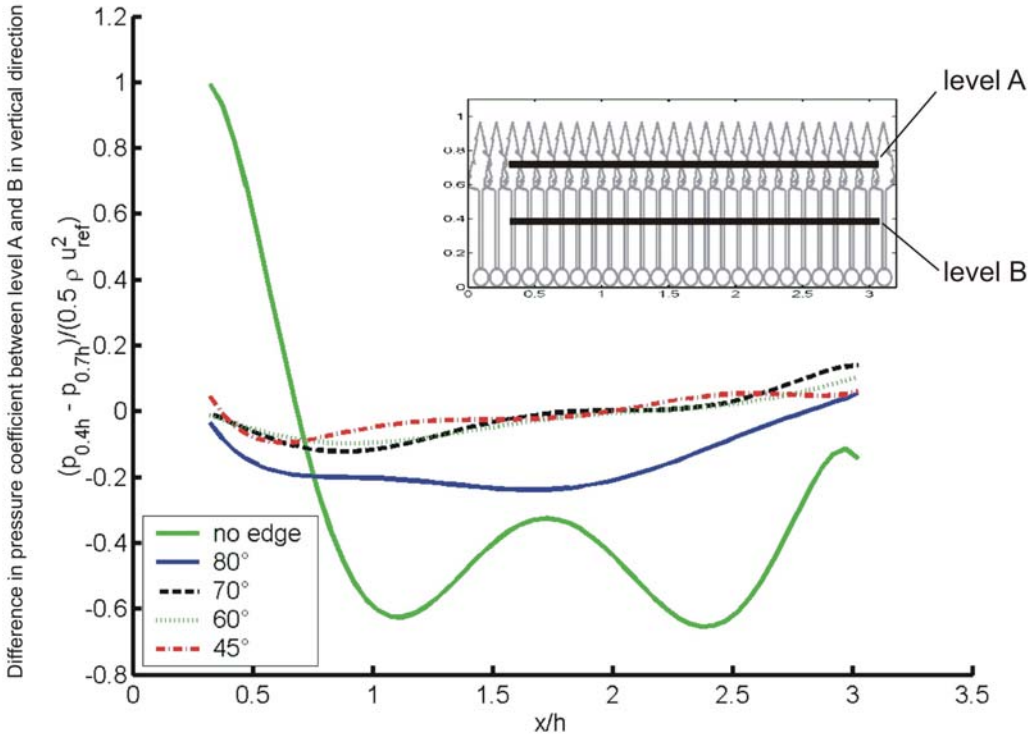

Figure 10. Pressure difference between trunk space (0.4h) and canopy (0.7h).

Discussion

The given pressure data clearly show the relationship between pressure pattern within the forest and the investigated parameters of edges, namely angle and porosity. Most interesting is the fetch x/h up to which higher pressure within the crown space occurs. At about this fetch, dynamic response of the trees could be observed, which may suggest coincidence with properties of the flow above the canopy (e.g. well-known maximum of turbulent shear stress, see also Ruck & Adams 1991), gust penetration and high wind loading. The forest edge zone is characterized by significant pressure gradients and wind loading on trees. So, the occurence of initial gaps in the canopy is likely under severe storm conditions, which then leads to failure of further trees experiencing high bending moments at the gap's surroundings (Fraser 1964). Initial gaps almost always preceeds catastrophic windthrow (Schmid-Haas & Bachofen 1991) in forests.

The data shown here were measured within a small forest stand, where effects occuring due to leading edge's properties might be superimposed by afflux due to the trailing edge. For a more precise investigation of the leading edge's influence on an extended forest, forest models of much longer extension should be investgated in the wind tunnel.

Vegetative canopies normally do not show sharp borders or geometric edges at all, but are highly flexible porous “bluff” bodies. The relationship between wind speed and permeability is crucial and variation of drag and permeability with wind speed is well-known (Mayhead 1973, Vogel 1993). Therefore, it is most likely that the findings are interchangeable within different vegetative canopies, however, a sophisticated scaling is required in order to fullfill similarity conditions.

The results shown in this paper are mean pressure values, integrated over 20 sec. Thus, the results are deduced from steady-state flow conditions. Further investigations are planned and will include time series analyses of pressure and wind velocity measured within and above the canopy to account for gust phenomena.

References

Agster, W. & B. Ruck 2002. Modellierung der Umströmung von Waldkanten in Windkanaluntersuchungen. Proceedings der 10. Jahrestagung der Deutschen Gesellschaft für Laser-Anemometrie GALA e.V., Rostock, pp. 37.1-37.7.

Counihan, J. 1969. An improved method of simulating an atmospheric boundary layer in a wind tunnel. Atmospheric Environment 3, 197-214.

Fraser, A. 1964. Wind tunnel and other related studies on coniferous trees and tree crops. Scottish Forestry 18, 84-92.

Fritzsche, K. 1933. Sturmgefahr und Anpassung: Physiologische und technische Fragen des Sturmschutzes. Tharandter Forstliches Jahrbuch 84(1), 1-94.

Hütte, P. 1967. Die standörtlichen Voraussetzungen der Sturmschäden. Forstwissenschaftliches Centralblatt 86, 276-295.

Irvine, M., B. Gardiner & M. Hill 1997. The evolution of turbulence across a forest edge. Boundary-Layer Meteorology 84, 467-496.

Mayhead, G. 1973. Some drag coefficents for british forest trees derived from wind tunnel studies. Agricultural Meterology 12, 123-130.

Morse, A., B. Gardiner & B. Marshall 2002. Mechanisms controlling turbulence development across a forest edge. Boundary-Layer Meteorology 103, 227-251.

Prien, S. & M. Leydolph 1974. Ursachen und begünstigende Faktoren für Sturmschäden im Mittelgebirge. Beiträge für die Forstwirtschaft 8(2), 69-76.

Ruck, B. & E. Adams 1991. Fluid mechanical aspects of the pollutant transport to coniferous trees. Boundary-Layer Meteorology 56, 163-195.

Schmid-Haas, P. & H. Bachofen 1991. Die Sturmgefährdung von Einzelbäumen und Beständen. Schweizerische Zeitschrift für Forstwesen 142(6), 477-504.

Schober, R. 1995. Ertragstafeln wichtiger Baumarten bei verschiedener Durchforstung (4th ed.). J.D. Sauerländer's Verlag, Frankfurt am Main.

Schretzenmayr, M., R. Haupt & T. Ullrich 1974. Zusammenhänge zwischen der Struktur des Waldrandes und dem Auftreten von Sturmschäden in der montanen Stufe des Ostharzes und sich daraus ergebende Hinweise zur Pflege der Waldränder. Sozialistische Forstwirtschaft 24, 116-120.

Shaw, R. 1977. Secondary wind speed maxima inside plant canopies. Journal of Applied Meteorology 16, 514-521.

Sigmon, J., K. Knoerr & E. Shaughnessy 1983. Microscale pressure fluctuations in a mature deciduous forest. Boundary-Layer Meteorology 27, 345-358.

Vogel, S. 1993. When leaves save the tree. Natural History 102(9), 58-62.

Vogl 1912. Wald und Sturm. Allgemeine Forst- und Jagd-Zeitung 88, 145-151.

von Fürst, H. 1912. Die Lehre vom Waldschutz (7th ed.). Verlagsbuchhandlung Paul Parey, Berlin.

Wangler, F. 1976. Die Sturmgefährdung der Fichte in Abhängigkeit vom Standort, Bestandestyp und Bestandeshöhe. Der Forst- und Holzwirt 31, 220-222.

Weihs, U., G. Wilhelm & R. Roos 1999. Wie sich unbehandelte Fichtenbestände aus Naturverjüngung entwickeln. AFZ/Der Wald 54(4), 172-175.